Quasifree scattering on clustering particles and separation energies*

Y. Sakamoto
Institut für Kernphysik der Universität Frankfurt am Main, Germany

P. Cüer
Laboratoire de Physique Corpusculaire, Centre de Recherches Nucléaires de Strasbourg, France

F. Takéutchi†
Institut für Experimentelle Kernphysik der Universität und des Kernforschungszentrums, Karlsruhe, Germany

(Received 15 October 1974)

The relation between cross sections for quasifree scattering on clustering particles and separation energies of the particles in light nuclei is investigated. When the wave function for the center of mass of clustering particles relative to that of remaining ones has an oscillatory structure in the interior region, the overlap integral contains only a small contribution from this region. Consequently, the dominant contribution to the cross section will come from the asymptotic part of the wave function, which essentially depends on the binding energy of the clustering particles in the nucleus. This is a common situation in many cases of quasifree scattering on clustering particles. A theory based on this approach is able to explain the large variation in the magnitudes of a number of measured quasifree scattering cross sections.

[NUCLEAR REACTIONS ^{6}Li(p,pd), $(p,p^3$He$)$, $(p,p\alpha)$, ^{7}Li(p,pd), (p,pt), ^{9}Be$(p,p\alpha)$, ^{12}C(p,pd), $E=155$ (100) MeV, calculated $\sigma(\theta)$; ^{6}Li$(\pi^-,2n)$, $E=0$ MeV, calculated recoil momentum distribution. Relation between the cross sections and separation energies.]

I. INTRODUCTION

The emission of α particles in interactions of high energy particles and absorption of pions by clustering particles in nuclei were noticed more than 20 years ago,[1] giving support for the α-particle model of light nuclei. More generally, the process of quasifree scattering (QFS) on composite particles in a reaction $A(x,xy)B$ has been extensively studied with the goal of extracting information about momentum components of the c.m. motion of clustering particles with respect to remaining particles, and about detailed clustering structure of particles in the nucleus.

Recently, data have been obtained for QFS on light nuclei, such as the ^{6}Li$(x,xd)^4$He reaction [see, for example, Ref. 2, where the data are tabulated for the ^{6}Li$(x,xd)^4$He reaction]. The data have been analyzed with the spectator model. By this model the cross section is essentially proportional to the square of the momentum wave function for the c.m. of the particles y relative to that of B in the nucleus A. In the analyses, the predicted results were multiplied by a factor for fitting with data in absolute units. This factor was called a "probability" of finding the particles y in the nucleus, or their effective number. Such a factor contains effects due to initial- and final-state interactions for incident and outgoing particles. It might happen that the probability, thus determined, depends on the type of projectile particle x and momenta of particles in the initial and final states. It depends also on the wave function chosen for describing the c.m. motion of y in A. In general the cross sections predicted with harmonic oscillator wave functions are too small, because of the incorrect asymptotic behavior of such functions. To improve this, many authors[4] use the method of joining an appropriate asymptotic function to harmonic oscillator functions in such a way that the logarithmic derivative varies slowly at the matching point. However, with such a wave function, the predicted cross sections are now too large (at least by a factor of 2) compared with data. In addition this arbitrary method is by no means reliable since these modified wave functions give rise to nuclear form factors different from those predicted with harmonic oscillator functions whose parameters are determined from electron scattering. Actually, the probability extracted from various data varies 0.035 (Ref. 3) to 1.6 (Ref. 4) for the breakup reaction of ^{6}Li into a deuteron and an α particle.

The QFS is dominated by low momentum components of the wave function. The low momentum components are correctly described by the asymptotic form of the wave function, which essentially depends on the separation energy of the particles.

Moreover, the wave function for the c.m. of clustering particles relative to that of remaining ones has usually an oscillatory structure, and hence the overlap integral is largely canceled for the interior region. Therefore, the cross section for QFS is explained by a simple parameter-free calculation in terms of the separation energy. The large variation of the clustering probability stated above is greatly reduced by taking into account the diminution of the overlap integral in the interior region. This has been demonstrated for the ^{6}Li-$(d, d\alpha)^2$H reaction.[2]

There exist some calculations[5] which include distortion effects for the incident and outgoing particles in QFS on clustering particles. However, even if the parameters of optical distortion potentials for the incident and outgoing particles are fixed from corresponding elastic scattering, a large number of these parameters makes insight into the QFS process difficult. Moreover, the calculated cross sections for QFS with high energy incident and outgoing particles depend essentially on the nuclear wave function chosen rather than on the optical potential with reasonable parameters.

We have shown[6] that the large difference between cross sections for QFS in the ^{6}Li(p, pd) and $(p, p^3\text{He})$ reactions is explained by a simple parameter-free calculation in terms of the separation energies of ^{6}Li into a deuteron and an α particle, and into a triton and a ^{3}He particle. The purpose of the present paper is to show that the bulk of the data for QFS on clustering particles in light nuclei can be explained in the same simple parameter-free calculation instead of the use of sophisticated models containing many adjustable parameters.

II. CALCULATIONS

A. Cross section for the quasifree scattering

The differential cross section for a three-particle final state is, in the laboratory system

$$d\sigma = \frac{(2\pi)^4}{|\vec{v}_{\text{rel}}|} d\vec{k}_x d\vec{k}_y d\vec{k}_B \times \delta(\vec{k}_0 - \vec{k}_x - \vec{k}_y - \vec{k}_B)\delta(E_i - E_f) \sum |T_{fi}|^2 , \quad (1)$$

where $\vec{k}_0$, $\vec{k}_x$, $\vec{k}_y$, and $\vec{k}_B$ are, respectively, the momenta of incident and scattered particle x, knocked-out particle y and residual nucleus B; $E_{i(f)}$ is the total energy of the system in the initial (final) state; T is the transition matrix element for the reaction, and $|\vec{v}_{\text{rel}}| = k_0/E_0$, E_0 being the total energy of particle x.

By assuming that the knockout process takes place in the collision between the incident particle x and clustering particles y in the nucleus, Eq. (1) is reduced to, in the impulse approximation,

$$\frac{d^3\sigma}{d\Omega^2 dE} = K|I(\vec{k}_0, \vec{k}_x, \vec{k}_y; \vec{k}_B)|^2 |t(\vec{k}_0, \vec{k}_x; \vec{k}_y)|^2 , \quad (2)$$

where K is the kinematical factor and I is the overlap integral which depends mainly on the total momentum transfer

$$\Delta\vec{k} = \vec{k}_0 - \vec{k}_x - \vec{k}_y = \vec{k}_B , \quad (3)$$

and on the momentum transfer in the x-y scattering system

$$\vec{q} = \vec{k}_0 - \vec{k}_x . \quad (4)$$

The function $t(\vec{k}_0, \vec{k}_x; \vec{k}_y)$ with $\vec{q} = \vec{k}_y$ represents the t matrix for the elementary process averaged over spin and isospin states of x particles and y nucleons, and is connected to the cross section for free x-y scattering by the relation

$$\left(\frac{d\sigma}{d\Omega}\right)^{\text{free}}_{x-y} \propto |F^{\text{fr}}_{xy}(\vec{q})t(\vec{q})|^2 , \quad (5)$$

where F^{fr}_{xy} is the product of the form factors for both the particles x and y. For example, in the case of the nucleon-deuteron scattering, $t(\vec{k}_0, \vec{k}_x; \vec{k}_y)$ is the two-nucleon t matrix averaged[7] over spin and isospin states of deuteron, and F^{fr}_{xy} is the deuteron form factor

$$F_d(\vec{q}) = \int e^{\frac{1}{2}i\vec{q}\cdot\vec{r}} |\psi_d(\vec{r})|^2 d\vec{r} . \quad (6)$$

Thus, the cross section can be written as,[8,9]

$$\frac{d^3\sigma}{d\Omega^2 dE} = K \left| \frac{I(\vec{k}_0, \vec{k}_x, \vec{k}_y; \vec{k}_B)}{F^{\text{fr}}_{xy}(\vec{q})} \right|^2 \left(\frac{d\sigma}{d\Omega}\right)^{\text{free}}_{xy} . \quad (7)$$

In the plane wave approximation, the function $I(k_0, k_x, k_y; k_B)$ is factorized as

$$I(\vec{k}_0, \vec{k}_x, \vec{k}_y; \vec{k}_B) = \sum_{yB} S_{yB} I_B(\vec{k}_0, \vec{k}_x, \vec{k}_y; \vec{k}_B) F_{xy}(\vec{q}) , \quad (8)$$

where S is the spectroscopic factor and $F_{xy}(\vec{q})$ is the product of the form factor of particle x and the overlap between the clustering particles y in the nucleus and free y particle. The ratio $F_{xy}(\vec{q})/F^{\text{fr}}_{xy}(\vec{q})$ depends on $\vec{q}$.[9] However, this dependence can be minimized by keeping $\vec{q}$ constant in the kinematics corresponding to the QFS.[10]

When the $\vec{q}$ dependence of $I(\vec{k}_0, \vec{k}_x, \vec{k}_y; \vec{k}_B)$ is assumed to be represented by an appropriate free x-y cross section $(d\sigma/d\Omega)_{x-y}$, Eq. (2) can be written in the so-called QFS model as[11]

$$\frac{d^3\sigma}{d\Omega^2 dE} = K' \left(\frac{d\sigma}{d\Omega}\right)_{x-y} |\Phi(\vec{k}_0, \vec{k}_x, \vec{k}_y; \vec{k}_B)|^2 . \quad (9)$$

In this equation the overlap integral Φ depends

mainly on $\Delta\vec{k}$ as given by Eq. (3), and is expressed in the distorted wave impulse approximation as

$$\Phi(\vec{k}_0, \vec{k}_x, \vec{k}_y; \vec{k}_B) = \langle \chi^{(-)}_{\vec{k}_x} \psi(\vec{\rho}_x) \chi^{(-)}_{\vec{k}_y} \psi(\vec{\rho}_y) \psi(\vec{\rho}_B) | \chi^{(+)}_{\vec{k}_0} \psi(\vec{\rho}_x) \Psi(\vec{\rho}_A) \rangle , \quad (10)$$

where $\chi^{(-)}_{\vec{k}_x}$, $\chi^{(-)}_{\vec{k}_y}$ are incoming distorted waves for the particles x and y, and $\chi^{(+)}_{\vec{k}_0}$ is an outgoing distorted wave for the particle x; $\psi(\vec{\rho}_x)$ and $\psi(\vec{\rho}_y)$ are internal wave functions for these particles, and $\Psi(\vec{\rho}_A)$ stands for the wave function of the target nucleus. In the plane wave approximation, Eq. (10) is reduced to

$$\Phi(\vec{k}_0, \vec{k}_x, \vec{k}_y; \vec{k}_B) \equiv \Phi(\Delta\vec{k}) = \frac{1}{(2\pi)^{3/2}} \times \int e^{i\Delta\vec{k}\cdot\vec{r}} \phi(\vec{r}) d\vec{r} , \quad (11)$$

where $\phi(\vec{r})$ is the wave function for the c.m. of clustering particles relative to that of remaining ones.

In Eq. (9), when $d\Omega^2 dE$ is given by $d\Omega_x d\Omega_y dE_x$ and $(d\sigma/d\Omega)_{x-y}$ is the appropriate c.m. cross section for the x-y scattering, K' is

$$K' = \frac{k_x k_y^2 E_B E_{\text{c.m.}}^2}{k_0 E_{y_i} [k_y E_B + E_y(k_y - k_0 \cos\theta_y + k_x \cos\theta_{xy})]} . \quad (12)$$

Here E_{y_i}, E_y, and E_B are, respectively, the total energies of the particle y in the initial and final states and that of B in the final state; $E_{\text{c.m.}}$ is the total energy in the c.m. x-y system; θ_y is the angle between $\vec{k}_0$ and $\vec{k}_y$; θ_{xy} is the angle spanned by $\vec{k}_x$ and $\vec{k}_y$.

B. Nuclear wave function

The wave function of the nucleus is written in the y-B cluster model as

$$\Psi = A\phi_y(\vec{\rho}_y)\phi_B(\vec{\rho}_B)\phi(\vec{r}) , \quad (13)$$

where ϕ_y and ϕ_B are, respectively, the internal wave functions of the clustering and remaining particles; $\phi(\vec{r})$ is the wave function for the c.m. of particles y with respect to that of remaining ones in the nucleus; and A is the antisymmetrization operator for particles in the nucleus. The radial and angular quantum numbers of $\phi(\vec{r})$ are obtained by imposing energy conservation on the shell model wave functions.

The antisymmetrized c.m. wave function of y is

$$\tilde{\phi}(\vec{r}) = \int \phi_y^*(\vec{\rho}_y)\phi_B^*(\vec{\rho}_B)\Psi d\vec{\rho}_B d\vec{\rho}_y , \quad (14)$$

which is easily expressed[12-14] in terms of Gaussian functions when ϕ_y, ϕ_B, and $\phi(\vec{r})$ are taken to have harmonic oscillator form. The difference between $\tilde{\phi}(\vec{r})$ and $\phi(\vec{r})$ is appreciable only in the region of small relative distance r.

Since QFS is dominated by low momentum components of nuclear wave functions, the asymptotic form of the functions is expected to have a large effect on the determination of the magnitude of observed cross sections. This is essential to reproduce the cross sections for reactions with small Q values such as QFS in $^6\text{Li}(p, 2p)^5\text{He}$.[15] Similarly, the asymptotic form of the c.m. wave function of y is expected to have a major influence on QFS in the more general reaction $A(x, xy)B$.

To take the asymptotic form correctly, we choose a sperical Hankel function

$$\phi(\vec{r}) = Bh_l^{(1)}(i\beta r) Y_{lm}(\hat{r}) , \quad r \geq R , \quad (15)$$

where

$$\beta = \sqrt{2\mu\epsilon} , \quad (16)$$

here μ is the reduced mass between the particles y and B, and ϵ is the separation energy of y in A.

When the function $\phi(\vec{r})$ has its radial quantum number n larger than 1, both $\phi(\vec{r})$ and $\tilde{\phi}(\vec{r})$ have an oscillatory behavior with n nodes. The oscillation of the functions is well localized in the interior region of a certain radius. The overlap integral is directly related to the wave function itself, as seen in Eq. (11). The oscillatory behavior of any function acts to diminish the contribution to the overlap integral in its oscillatory region. Therefore the main contribution to the integral comes from the function in the region of large r where there is almost no difference between $\phi(\vec{r})$ and $\tilde{\phi}(\vec{r})$. This means that the oscillatory behavior of $\phi(\vec{r})$ makes the antisymmetrization effects less important in the overlap integral. Moreover, the absorption effects for incident and outgoing particles due to the target and residual nucleus act to attenuate the overlap integral in the region of small r. This also makes the antisymmetrization effects less important. When the cutoff approximation is employed with the assumption of strong absorption for the incident and outgoing particles, antisymmetrization has a negligible effect on the overlap integral.

Therefore to determine the constant B, Eq. (15) is joined with a spherical Bessel function

$$\phi(\vec{r}) = Aj_l(\alpha r) Y_{lm}(\hat{r}) , \quad r < R \quad (17)$$

at $r = R$. The constants A, B, and α are determined by requiring the continuity condition for the logarithmic derivative of $\phi(\vec{r})$ at $r = R$ and the normalization condition. The constant α is fixed so that $j_l(\alpha r)$ has the same number of nodes as $\tilde{\phi}(\vec{r})$ inside $r < R$.

III. RESULTS

To evaluate Eq. (10), one needs distorted waves due to optical potentials. However, optical potentials to describe interactions between a nucleon and very light nuclei such as a deuteron are not clear. For the wave function with nodes, the cancellation occurs in the overlap integral for the interior region where nuclear absorption effects are expected to be important. This cancellation diminishes nuclear absorption effects. Therefore, instead of the use of distorted waves which are subject to serious criticism for very light nuclei, Eq. (11) is used in the present calculations for demonstrating how the magnitudes of a number of measured QFS cross sections are accounted for in terms of the corresponding separation energies.

The present calculations are entirely parameter free except for the choice of the radius R. However, this choice of R is not essential as shown later.

We have also calculated the cross sections with the cutoff approximation, supposing the case of extremely strong absorption for the incident and outgoing particles. The cutoff radius R_c is taken to be equal to the radius R. The difference between the results calculated with and without the cutoff approximation is found to be small for small ϵ values. This gives also a support for the present parameter-free calculations.

A. Values used in the calculations for cross sections

1. Nuclear radius

In the present calculations the radius $R = 3.5$ fm is used regardless of sizes of target nuclei, to demonstrate how the cross sections for the QFS depend on the values of ϵ. It should be noted, of course, that the absolute values of the calculated cross sections do depend on the values chosen for R. However, when R varies by ± 0.5 fm from the used value, the absolute cross sections calculated without the cutoff approximation change by only a small amount, at most within the size of the experimental error bars. The results with the cutoff approximation are even less sensitive to variation in R. This is especially the case for calculated cross sections for the reactions involving large ϵ values. Moreover, the ratio between the calculated cross sections for QFS in such reactions as ^{6}Li-$(p, pd)^4$He and ^{6}Li$(p, p^3\mathrm{He})^3$H at $\Delta\vec{k} = 0$ is insensitive to the chosen value of R.

The square well function may be suspected not to reproduce the form factor obtained from electron scattering data. However, for small momentum transfers where the QFS process dominates, the form factor can be expanded as

$$F(\vec{q}) = \int \rho(\vec{r}_A) e^{i\vec{q}\cdot\vec{r}_A} d\vec{r}_A = 1 - \tfrac{1}{6}\langle \vec{r}_A^{\,2}\rangle \vec{q}^{\,2} + \cdots , \quad (18)$$

where $\rho(\vec{r}_A)$ is the nuclear density distribution, $\vec{q}$ being the momentum transfer. The rms radius $\langle \vec{r}_A^{\,2}\rangle^{1/2}$ of the nucleus can be expressed in terms of an average distance $\langle \vec{r}_{yB}^{\,2}\rangle^{1/2}$ between the c.m. of clustering particles y and that of the remaining ones B, and rms radii of these clustering and remaining particles, y and B. For example the rms radius of ^{6}Li for the d-α configuration is given by

$$\langle \vec{r}_{^6\mathrm{Li}}^{\,2}\rangle = \tfrac{2}{9}\langle \vec{r}_{d\alpha}^{\,2}\rangle + \tfrac{1}{12}\langle \vec{\rho}_d^{\,2}\rangle + \tfrac{2}{3}\langle \vec{\rho}_\alpha^{\,2}\rangle , \quad (19)$$

where $\langle \vec{r}_{d\alpha}^{\,2}\rangle^{1/2}$ is the average d-α separation, $\langle \vec{\rho}_d^{\,2}\rangle^{1/2}$ is the average distance between two particles (that is, twice the rms radius of the deuteron cluster), and $\langle \vec{\rho}_\alpha^{\,2}\rangle^{1/2}$ is the rms radius of the α-particle cluster. Therefore the rms radius of the nucleus is not fixed only by $\langle \vec{r}_{yB}^{\,2}\rangle$. It can be possible that a small variation of $\langle \vec{r}_{yB}^{\,2}\rangle$ can be compensated by slight changes of $\langle \vec{\rho}_y^{\,2}\rangle$ and/or $\langle \vec{\rho}_B^{\,2}\rangle$ to keep $\langle \vec{r}_A^{\,2}\rangle$ consistent with that observed, although length parameters of clustering particles for light nuclei are not expected to differ very much from those of corresponding free particles. Such small changes of rms radii of clustering particles hardly affects the QFS cross section calculated with the spectator model.

The form factor does not depend sensitively on details of the wave function of the c.m. of clustering particles for small momentum transfers, and hence can give only a loose restriction on the choice of R through the rms radius of the nucleus.

2. Normalization of wave function

The normalization of the wave function for the c.m. of clustering particles with respect to that of remaining ones in Li nuclei is not take to be unity in the present calculation,

$$c^2 = \int |\phi(\vec{r})|^2 d\vec{r} \neq 1 . \quad (20)$$

This is due to the following reason: Even if the wave functions $\phi(\vec{r})$, $\phi_y(\vec{\rho}_y)$, and $\phi_B(\vec{\rho}_B)$ in Eq. (13) are normalized to be unity, the antisymmetrized wave function $\tilde{\phi}(\vec{r})$ given by Eq. (14) has not in general the normalization factor which gives unity,

$$\theta^2 = \int |\tilde{\phi}(\vec{r})|^2 d\vec{r} \neq 1 . \quad (21)$$

The factor θ^2 is easily calculated,[14] if the functions $\phi(\vec{r})$, ϕ_y, and ϕ_B are taken to have harmonic oscillator form. We use this factor θ^2 calculated with harmonic oscillator functions as the normalization

factor c^2 in the present calculation for cross sections for breakup reactions of the Li nucleus.

Although the factor c^2 can be similarly determined for the c.m. wave functions of clustering particles in nuclei such as ^{9}Be and ^{12}C considered here, for these nuclei the fractional parentage coefficients for clustering configurations[16] predicted with shell model calculations are used to determine c^2.

It should be noted that the factor c^2 determined from the fractional parentage coefficients can differ in general from θ^2 determined with harmonic oscillator cluster model functions. For example the squares of the fractional parentage coefficients in the shell model are $\frac{9}{8}$ and $\frac{8}{9}$[14,17] for d-α and t-^{3}He configurations in the ^{6}Li ground state. On the other hand, the factors 1.07 and 0.6 are the most probable[14] for the d-α and t-^{3}He systems in the harmonic oscillator cluster model wave functions of ^{6}Li. These differences are due to the fact that in the shell model a single common parameter is used for the functions $\phi(\vec{r})$, $\phi_y(\vec{\rho}_y)$, and $\phi_B(\vec{\rho}_B)$, in contrast with the cluster model where these functions have, respectively, their own parameters.

It is assumed in the present calculation that the overlap between the internal wave functions of clustering particles and the remaining ones $\phi_y(\vec{\rho}_y)\phi_B(\vec{\rho}_B)$ and these of corresponding free particle and residual nucleus $\Psi_y(\vec{\rho}_y)\Psi_B(\vec{\rho}_B)$ is unity, although it is generally less than unity.

3. *x-y scattering cross section*

Experimental uncertainties, for the time being, mask off-the-energy shell effects on $(d\sigma/d\Omega)_{x-y}$, although the effects become appreciable for the cross sections of QFS involving large $\Delta\vec{k}$ values. An off-the-energy shell cross section takes its value between the on-the-energy shell cross sections at the relative energies E^i_{x-y} and E^f_{x-y} of the x-y system in the initial and final states.[18] It is assumed that there is no resonance state of that system in the energy range between the E^i_{x-y} and E^f_{x-y}. The energy difference $E^i_{x-y} - E^f_{x-y}$ is small for the QFS kinematical region with small $\Delta\vec{k}$ values. The difference between on-the-energy shell cross sections at E^i_{x-y} and E^f_{x-y} is also small for high energy projectiles.

Therefore, when experimental conditions for QFS are chosen so that the relative energies E^i_{x-y} and E^f_{x-y} are high, then the cross section $(d\sigma/d\Omega)_{x-y}$ is well approximated by the cross section for free x-y scattering, $(d\sigma/d\Omega)^{\text{free}}_{x-y}$, under the additional conditions: (1) that incident and transferred momenta involved in $(d\sigma/d\Omega)^{\text{free}}_{x-y}$ are chosen to be the same as those in $(d\sigma/d\Omega)_{x-y}$, and (2) that there is no resonance state of the x-y system in the energy range between E^i_{x-y} and E^f_{x-y}. In the present calculations $(d\sigma/d\Omega)^{\text{free}}_{x-y}$ are taken from Ref. 19.

B. Breakup of Li

1. *^{6}Li(x,xd)^{4}He and ^{6}Li(x,x α)^{2}H reactions*

Figure 1 shows the calculated results compared with data[20] for QFS in the ^{6}Li$(p,pd)^4$He reaction at an incident proton energy of 156 MeV. The function $\phi(\vec{r})$ is a $2S$ state. The absorption effects for incident and outgoing particles due to the nuclear potential are usually taken into account with the cutoff approximation. This treats the nucleus as being completely black inside the cutoff radius. The dashed curve is calculated with the cutoff approximation. The solid curve includes the contribution from $\phi(\vec{r})$ for $r < R$. The difference between both the curves is small. The function for $r < R$ does not strongly contribute to the overlap integral because of its oscillatory structure. This diminution of the overlap integral for the interior region is typical for the functions of small separation energy ϵ. The cross sections for the different kine-

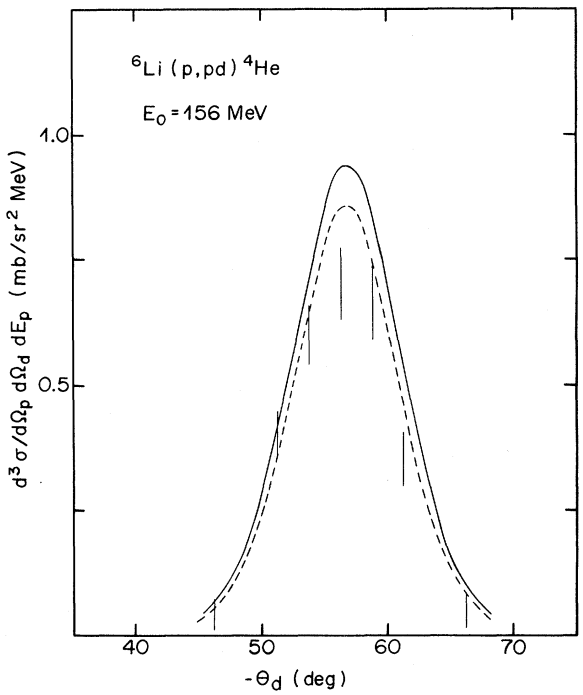

FIG. 1. The correlation cross section for the ^{6}Li$(p,pd)^4$He reaction at 156 MeV incident proton energy for a detection angle of scattered protons $\theta_p = 43.6°$ with its energy $E_p = 113$ MeV. The dashed and solid curves are calculated, respectively, with and without the cutoff approximation. The radius of the square well and the cutoff radius for the asymptotic function are taken to be $R = 3.5$ fm for the $2S$ state function.

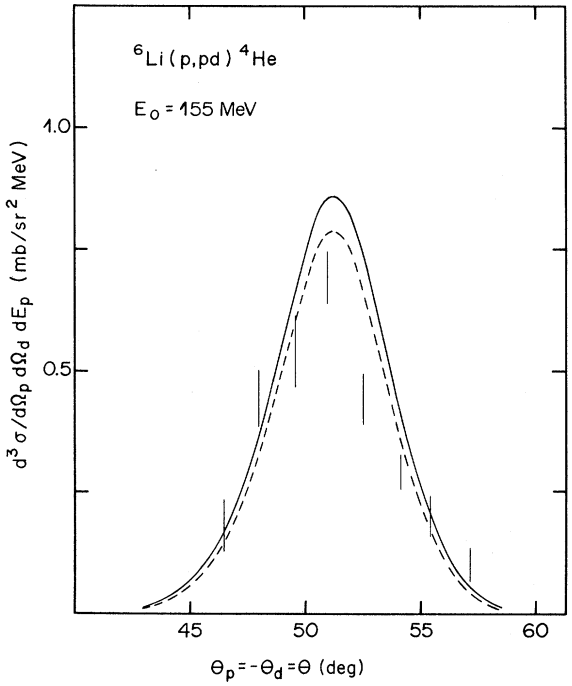

FIG. 2. The correlation cross section for the ^{6}Li$(p,pd)^4$He reaction at 155 MeV incident protons for $\theta_p = -\theta_d$ and $|\vec{k}_p| = |\vec{k}_d|$. The curves correspond to those in Fig. 1.

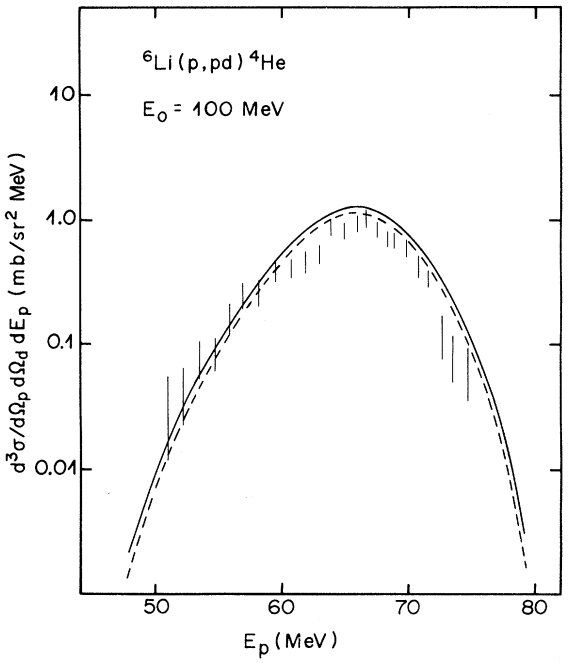

FIG. 3. The correlation cross section for the ^{6}Li$(p,pd)^4$He reaction at 100 MeV incident protons for $\theta_p = -\theta_d = 51.5°$. The curves correspond to those in Fig. 1.

matical conditions and energies are shown in Figs. 2 and 3 in comparison with data.[21,22]

Figure 4 shows the comparison between the observed[21] and calculated correlation cross sections for the ^{6}Li$(p, p\alpha)^2$H reaction at 155 MeV incident protons. This reaction is complementary to the ^{6}Li$(p, pd)^4$He reaction. The overlap integral is common for both the reactions if the approximation used is valid. The comparison of the cross sections for both the reactions serves to check the validity of the approximation.

2. ^{7}Li(p,pt)^{4}He reaction

The small overlap integral for $r < R$ is also seen for wave functions with nonzero angular momentum. In particular, Fig. 5 shows the results compared with data[20] for the ^{7}Li$(p, pt)^4$He reaction at 156 MeV incident proton energy, where the wave function $\phi(\vec{r})$ is a $2P$ state. The dashed and solid curves are calculated, respectively, with and without the cutoff approximation at $R_c = R$. The contribution from $r < R$ is small. The cross section is proportional to $\Delta\vec{k}^2$ for small momentum transfers $\Delta\vec{k}$ and is suppressed around the kinematical region corresponding to the QFS.

3. ^{6}Li(p,p^{3}He)^{3}H reaction

The cross section for the ^{6}Li$(p, p^3\mathrm{He})^3$H reaction is calculated as an example involving a large value

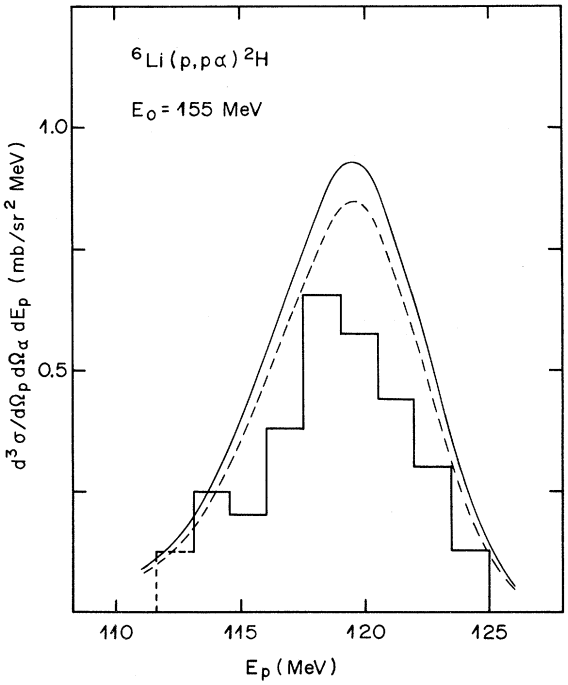

FIG. 4. The correlation cross section for the ^{6}Li$(p,p\alpha)^2$H reaction at 155 MeV incident protons for $\theta_p = -\theta_\alpha = 55°$. The curves correspond to those in Fig. 1.

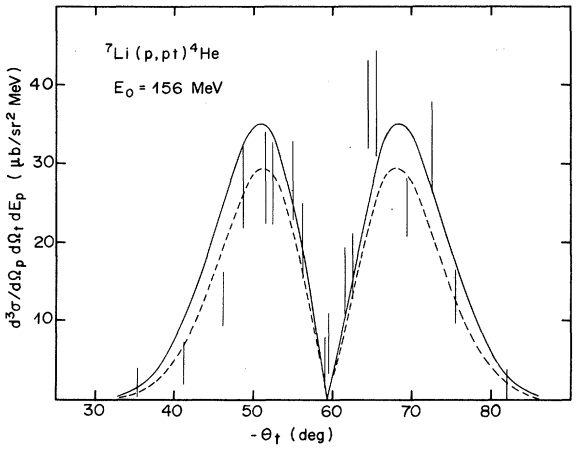

FIG. 5. The correlation cross section for the ^{7}Li(p,pt)^{4}He reaction at 156 MeV incident protons for $\theta_p = 44.6°$ and $E_p = 123.7$ MeV. The dashed and solid curves are calculated, respectively, with and without the cutoff approximation. The $2P$ state wave function with $R = 3.5$ fm is used.

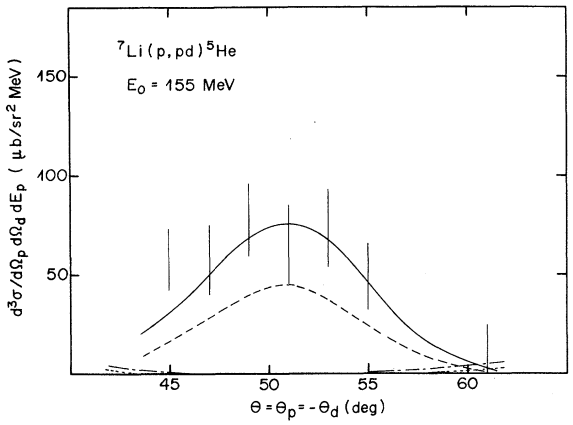

FIG. 7. The correlation cross section for the ^{7}Li(p,pd)^{5}He reaction at 155 MeV incident protons for $\theta_p = -\theta_d$ and $|\vec{k}_p| = |\vec{k}_d|$. The dashed and solid curves are calculated, respectively, with and without the cutoff approximation for the $2S$ state wave function. The dotted and dot-dashed curves stand for the results calculated with and without the cutoff approximation for the $1D$ state wave function. $R = 3.5$ fm is used for both the wave functions.

of ϵ. Figure 6 shows the results compared with data[20,23] for the QFS at 156 MeV incident protons. The wave function $\phi(\vec{r})$ is a $2S$ state. The wave function falls off rapidly in the exterior region and is consequently enhanced in the interior region because of the large ϵ value. The overlap integral for $r < R$ is nearly equal to that for $r > R$. The contribution from $\phi(\vec{r})$ for $r < R$ is not negligible and therefore the method proposed here gives much better results than the cutoff method.

4. ^{7}Li(p,pd)^{5}He reaction

Figure 7 shows the results compared with data[21] for the ^{7}Li(p,pd)^{5}He reaction at 155 MeV incident protons. The function $\phi(\vec{r})$ is a superposition of the $2S$ and $1D$ states with nearly equal weight. However, the cross section is strongly suppressed by a factor of $\Delta\vec{k}^4$ in the kinematical region of small $\Delta\vec{k}$ for the D state wave function. The D state contribution becomes appreciable when $\Delta\vec{k}$ becomes large. It is comparable with that of the S state around $|\Delta\vec{k}| = 100$ MeV/c. The S state contribution dominates for predicting the correlation cross section in its shape as well as in the absolute values for the QFS of small $\Delta\vec{k}$. It is thus

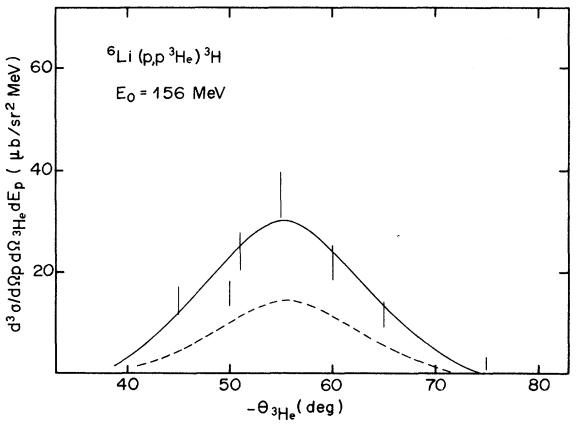

FIG. 6. The correlation cross section for the ^{6}Li(p,p^3He)^{3}H reaction at 156 MeV incident protons for $\theta_p = 46.2°$ and $E_p = 110$ MeV. The $2S$ state wave function with $R = 3.5$ fm is used. The curves correspond to those in Fig. 1.

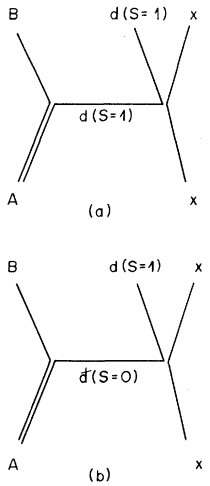

FIG. 8. The diagrams for the emission of two particles. The triplet to triplet states (a) and singlet to triplet states (b) transitions by the spin-dependent interactions.

hardly expected that any dip appears in the correlation cross section as a result of the D state contribution, although such a dip around $\Delta\vec{k}=0$ was predicted by some authors.[24]

A proton-neutron pair in a triplet spin state is emitted as a deuteron. However, it should be noted that a pair of particles in a singlet spin state can also be emitted[25] as a deuteron after the collision through spin dependent interactions, as shown in Fig. 8(b). Both processes occur coherently in the $^7\mathrm{Li}(p,pd)^5\mathrm{He}$ reaction. When two particles are knocked out as a deuteron from the three-particle system which consists of two neutrons in the singlet spin state $\chi_0(12)$ and a proton in its spin state $\chi_{1/2}(3)$, the amplitude is proportional to

$$\left\langle \sum_{\substack{j,k=1\\ j\neq k}}^{2} \chi_{1m}(j3)\tau_0(j3)\chi_{1/2}(k)\tau_{1/2}(k)\chi_{1/2}(p)\tau_{1/2}(p)\left|\sum_{i=1}^{3} t_{pi}\right|\chi_0(12)\tau_{1-1}\chi_{1/2}(3)\tau_{1/2}(3)\chi_{1/2}(p)\tau_{1/2}(p)\right\rangle , \tag{22}$$

where t_{pi} is the scattering spin matrix[26] between the incident and ith nucleon in the system, $\chi_{1/2}(p)$ is the spin function of the incident and scattered proton, $\chi_{1m}(j3)$ $(j=1,2)$ are the triplet spin functions of the emitted deuteron, $\chi_{1/2}(k)$ $(k=1,2;k\neq j)$ is the spin function of the remaining nucleon, and the symbols τ stand for the isospin functions for these particles. The amplitude is estimated in the same way as used[7] for calculating the cross sections for the elastic and inelastic scattering of nucleons by deuterons.

The use of a free scattering cross section $(d\sigma/d\Omega)_{p-d}$ takes account only of the transition for the process shown in Fig. 8(a). The results shown in Fig. 7 contain the contribution from both the processes. However, the cross section for the singlet to triplet process is small compared with that for the triplet to triplet process.

C. $^9\mathrm{Be}(p,p\alpha)^5\mathrm{He}$ reaction

The correlation cross section for QFS in the $^9\mathrm{Be}(p,p\alpha)^5\mathrm{He}$ reaction is compared with data[21] at 155 MeV incident protons in Fig. 9. Both $3S$ and $2D$ states are possible for the c.m. motion of the α clustering particles. Both wave functions have an oscillatory structure in the interior region. The dashed and solid curves are calculated, respectively, with and without the cutoff approximation at $R_c=R$ for only the $3S$ state wave function. The contribution from $r<R$ is seen to be small. The cross section for the $2D$ state is strongly suppressed by $\Delta\vec{k}^4$ in the kinematical region corresponding to the QFS. The predicted value is very small in the relevant region of $\Delta\vec{k}$ and has not been shown in Fig. 9.

D. $^{12}\mathrm{C}(p,pd)^{10}\mathrm{B}$ reaction

The cross sections for the $^{12}\mathrm{C}(p,pd)^{10}\mathrm{B}$ reaction at 156 MeV incident protons are predicted in Figs. 10 and 11 for the first and third excited states, respectively, of the residual nucleus. The reaction involves large ϵ value. When the residual nucleus is left in its ground state with $J=3^+$, the function $\phi(\vec{r})$ should have its angular momentum larger than $l=2$, since the contribution of the D state deuteron is neglected. The cross section is strongly hindered by a factor of $\Delta\vec{k}^{2l}$ in the kinematical region of the QFS. When the reaction leads to the residual nucleus left in its first and third excited states with $J=1^+$, the wave function $\phi(\vec{r})$ is the superposition of the $2S$ and $1D$ states, and of these, the $2S$ state is to make the largest contribution to the cross sections.

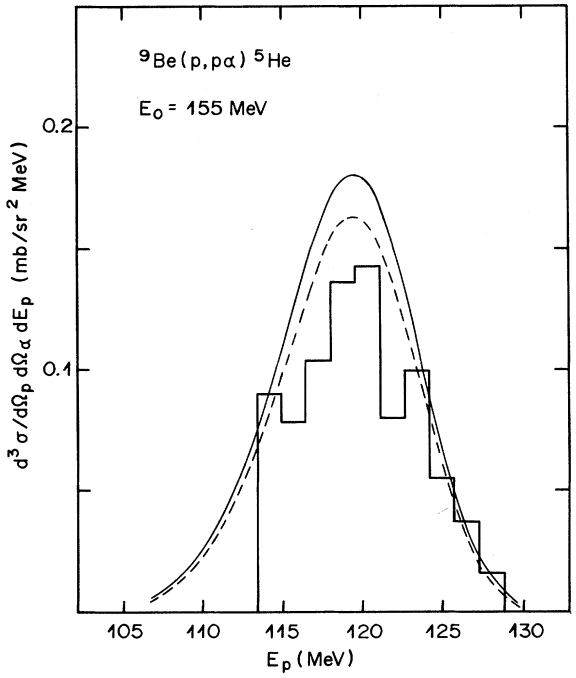

FIG. 9. The correlation cross section for the $^9\mathrm{Be}(p,p\alpha)^5\mathrm{He}$ reaction at 155 MeV incident protons for $\theta_p=-\theta_\alpha=55°$. The dashed and solid curves are calculated, respectively, with and without the cutoff approximation for the $3S$ state wave function with $R=3.5$ fm.

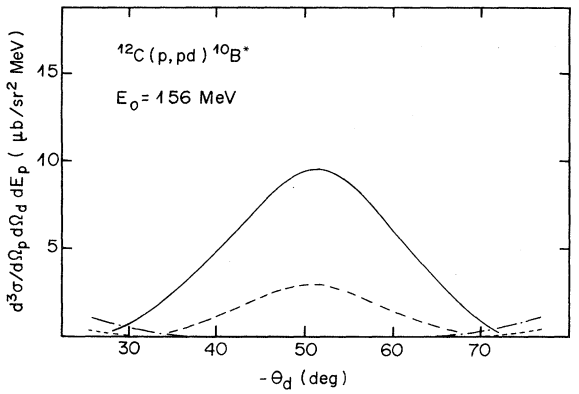

FIG. 10. The predicted correlation cross section for the $^{12}C(p,pd)^{10}B$ (first excited state) reaction at 156 MeV incident protons for $\theta_p = 41°$ and $E_p = 94.8$ MeV. $R = 3.5$ fm is used. The curves correspond to those in Fig. 7.

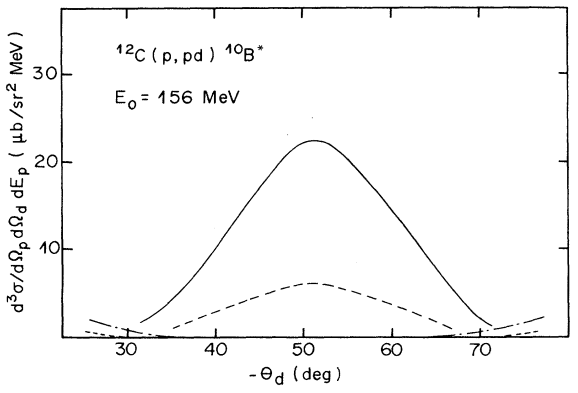

FIG. 11. The predicted correlation cross section for the $^{12}C(p,pd)^{10}B$ (third excited state) reaction at 156 MeV incident protons for $\theta_p = 41°$ and $E_p = 94.8$ MeV. The curves correspond to those in Fig. 7.

Bachelier[20] has measured the excitation energy spectra $d^4\sigma/d\Omega_p d\Omega_d dE_p dE_x$ of the ^{10}B residual nucleus for some pairs of detection angles. The correlation cross sections are estimated by integrating the spectra over the excitation energy E_x around the excited state under consideration. They lie between the values predicted with and without the cutoff approximation. The interior wave function affected with the nuclear volume absorption for the incident and outgoing particles acts also to account for the cross section, since the wave function does not extend appreciably outside the nuclear potential, due to the large ϵ values.

E. $^{12}C(p,pd)^{10}B^*$ (2nd ex.)—spin-isospin flip process

When the knockout process shown in Fig. 8(b) occurs on the nucleus of $J = 0^+$, $T = 0$, leaving the residual nucleus in the $J = 0^+$, $T = 1$ state, the correlation cross section for the QFS can show a peak around $\Delta\vec{k} = 0$. This is expected for the p-d QFS in ^{12}C with the residual ^{10}B nucleus left in its second excited state. However, the observed excitation energy spectra do not clearly show[20] such a peak.

This is understood as follows: The reaction occurs through the spin-dependent interaction and corresponds to the charge-exchange reaction by nucleons on nuclei with the transitions of $J = 0^+$ to 1^+ and 1^+ to 0^+. The cross section for the reaction with a spin-flip is smaller than that for the reaction with both spin-flip and non-spin-flip processes. This is seen[27] in the cross sections for the $^{14}N(p,n)^{14}O_{(g.s.)}$ and $^{18}O(p,n)^{18}F_{(g.s.)}$ reactions which are smaller than those for the $^{13}C(p,n)^{13}N_{(g.s.)}$ and $^{11}B(p,n)^{11}C_{(g.s.)}$ reactions by one to two orders of magnitudes at 150 MeV. The small cross section for the $^6Li(p,p')^6Li^*(T=1)$ reaction[28] also indicates that the spin-flip amplitude is small except for forward angles. Therefore we expect that such a QFS cross section for the transition with $\Delta T = 1$ between the target and residual nucleus is smaller than a QFS cross section with $\Delta T = 0$ by one to two orders of magnitudes, unless the fractional parentage coefficient involved in the $\Delta T = 1$ transition is so large as to compensate the small spin-isospin flip cross section.

The small cross section can be directly confirmed with a calculation similar to that given by Eq. (22), although the cross section for the $p + \vec{d}(S=0) \to p + d$ scattering cannot be obtained with usual scattering experiments. With the same notation used in Eq. (22), the amplitude for this process is proportional to

$$\left\langle \chi_{1m}(12)\tau_0(12)\chi_{1/2}(p)\tau_{1/2}(p) \left| \sum_{i=1}^{2} t_{pi} \right| \chi_0(12)\tau_{10}(12)\chi_{1/2}(p)\tau_{1/2}(p) \right\rangle \tag{23}$$

which gives a small cross section compared with that for the p-d elastic scattering.

The above argument can also be applied to explain the small contribution from the spin-dependent term in the $^7Li(p,pd)^5He$ reaction.

F. $^6Li(p,pd)^4He^*$—nodeless wave function

When the wave function has no node, there is a large difference between the overlap integrals calculated with and without the cutoff approximation.

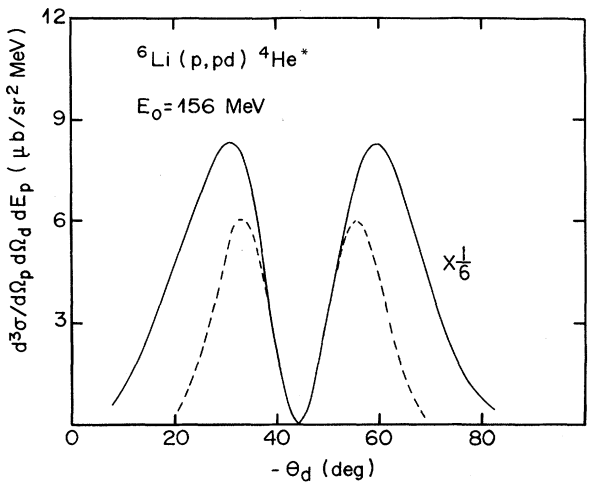

FIG. 12. The predicted correlation cross section for the ^{6}Li$(p,pd)^4$He reaction at 156 MeV incident protons for $\theta_p = 56°$ and $E_p = 78.5$ MeV, with the residual nucleus left in the negative parity states around 22 MeV excitation. The dashed and solid curves are calculated with and without the cutoff approximation for the $1P$ state wave function. $R = 3.5$ fm is used. The solid curve is multiplied by a factor $\frac{1}{6}$.

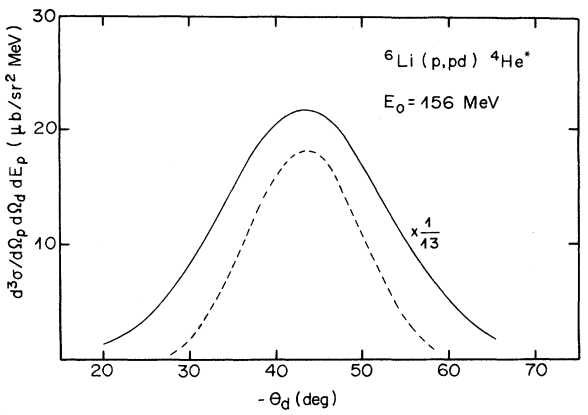

FIG. 13. The predicted correlation cross section for the ^{6}Li$(p,pd)^4$He reaction at 156 MeV incident protons for $\theta_p = 56°$ and $E_p = 75.6$ MeV, with the residual nucleus left in the positive states around 26 MeV excitation. The dashed and solid curves are calculated with and without the cutoff approximation for the $1S$ state. $R = 3.5$ fm is used. The solid curve is multiplied by a factor of $\frac{1}{13}$.

The difference becomes larger as the value of ϵ becomes larger. The nodeless wave function is associated, in general, with a large value of ϵ. As examples of this effect cross sections are predicted in this section for the QFS in the ^{6}Li$(p,pd)^4$He reaction, where the residual nucleus is left in its excited states.

The separation energy ϵ is about 22 MeV for removing two particles as a deuteron, one from the S shell and the other from the P shell, that is, one from the α cluster and the other from the deuteron cluster. The wave function $\phi(\vec{r})$ is a $1P$ state, so that the correlation cross section will show a minimum around $\Delta\vec{k} = 0$. Figure 12 shows the calculated cross sections summed over negative parity states around 23 MeV excitation of the residual ^{4}He nucleus.

The energy ϵ is in the region of 26 MeV for removing two particles as a deuteron from the S shell, that is, from the α-particle cluster. The wave function is a $1S$ state. The correlation cross section shows a maximum around $\Delta\vec{k} = 0$. Figure 13 shows the calculated cross sections summed over positive parity states with excitations higher than 26 MeV in the residual ^{4}He nucleus.

The large ϵ values lead to small cross sections. Such cross sections have not yet been observed with high precision. It is interesting to note how nuclear absorptions attenuate the overlap integral.

G. Knockout of α particles from heavier nuclei

The cross sections for QFS on α clustering particles in medium and heavier α-particle nuclei such as ^{24}Mg, ^{28}Si, ^{40}Ca, ^{140}Ce, and ^{232}Th have been found[29] to be smaller than that of ^{6}Li by a factor of 1/50 to 1/100, when the residual nuclei are left in the ground and lower excited states. These remarkably small cross sections are easily understood by the separation energies of α particles from the nuclei and by the fact that their reduced masses become larger as the mass of the nucleus increases. The case of ^{232}Th, however, requires some special considerations.

The c.m. wave functions of the clustering particles for such nuclei have large radial quantum numbers when the residual nuclei are left in their ground and lower excited states. The overlap integral for the interior region is strongly diminished by the oscillatory structure of the wave functions, so that the cross sections for QFS should be largely due to the asymptotic part of the wave functions. The correlation cross sections divided by

$$K'\left(\frac{d\sigma}{d\Omega}\right)_{x-y}$$

are

$$\frac{d^3\sigma}{d\Omega_x d\Omega_y dE_x}\Big/K'\left(\frac{d\sigma}{d\Omega}\right)_{x-y}\Bigg|_{\Delta\vec{k}=0} \begin{cases} \propto \dfrac{1}{(\mu\epsilon)^{3/2}} f(\sqrt{\mu\epsilon}\,R) & (\text{for } l=0) \\ =0 & (\text{for } l\neq 0) \end{cases}, \tag{24}$$

where l is the angular momentum for the c.m. of clustering particles with respect to that of remaining particles in the nucleus and $f(\sqrt{\mu\epsilon}\,R)$ is a factor which weakly depends on the radius R. The values estimated with Eq. (24) for ^{24}Mg, ^{28}Si, ^{40}Ca, and ^{140}Ce are, at least, smaller than that for ^{6}Li by an order of magnitude.

For heavier nuclei with $Z \ll A - Z$, the protons which make up an α-particle cluster with neutrons are in different shells from those occupied by the neutrons. This also decreases the possibility of α-particle clustering. The internal wave function of clustering particles $\phi_y(\vec{\rho}_y)$ can be considerably different from that of the free particle $\psi_y(\vec{\rho}_y)$, compared with the case for light nuclei.

Thus, the cross sections for the α-particle knockout reaction are hindered by the large ϵ values even for the α-particle nuclei. In other words, the cross sections are small because of tightly bound α-particle nuclei.

One might think that the present method cannot be applied in explaining the cross section for α particles knocked out from ^{232}Th, since this nucleus is radioactive for the α decay. However, its high Coulomb barrier prevents the separation of an α particle from the nucleus. The c.m. wave function of the α clustering particles is chosen so that it is confined by the Coulomb barrier, in spite of the positive Q value. The cross section is expected to be very small for knocked-out α particles with kinetic energies below the barrier.

H. ^{6}Li(π^-, $2n$)^{4}He reaction

It is worthwhile to see how well the wave function used for explaining data from a $A(x, xy)B$ reaction reproduces momentum distributions obtained from a pion absorption process $A(\pi, y')B$. For the absorption by clustering particles the matrix element is associated, in general, with the c.m. as well as relative wave functions of the particles.

As an example the recoil momentum distributions of ^{4}He are calculated for the ^{6}Li(π^-, $2n$)^{4}He reaction. The pion is assumed to be absorbed from its S orbit, the atomic number of ^{6}Li being small. The transition matrix element is proportional to[30]

$$\Phi(\vec{k})\varphi(\vec{\kappa})\vec{\kappa}, \tag{25}$$

where $\vec{k}$ and $\vec{\kappa}$ are, respectively, the c.m. and relative momenta of the two particles which participate in the absorption. With the plane wave approximation, the c.m. momentum function $\Phi(\vec{k})$ is the Fourier transform of the wave function given by Eqs. (15) and (17). To estimate the contribution of the relative wave function to the recoil momentum distributions, the relative momentum function $\varphi(\vec{\kappa})$ is taken to be the Fourier transform of a simple Gaussian function

$$\varphi(\vec{\kappa}) = \frac{1}{(2\pi)^{3/2}} \int \left[N \exp\left(-\frac{1}{4b^2}\vec{\rho}^{\,2}\right) Y_{00}(\hat{\rho})\right] e^{i\vec{\kappa}\cdot\vec{\rho}}\, d\vec{\rho}, \tag{26}$$

where $\vec{\rho}$ is the relative distance between the two particles. The length parameter b can be adjusted so that the functions (15), (17), and (26) can reproduce electron scattering data. For the purpose of estimating effects due to the relative wave functions, $b = 2.24$ and 1.72 fm[31] are used, respectively, for particles in the P and S shells. If the absorption is assumed to occur at zero range for the two particles, the transition matrix element is proportional to

$$\Phi(\vec{k})\vec{\kappa}. \tag{27}$$

Energy conservation requires

$$E_\pi + E_{\mathrm{Li}} = E_{^4\mathrm{He}} + E_{n_1} + E_{n_2}, \tag{28}$$

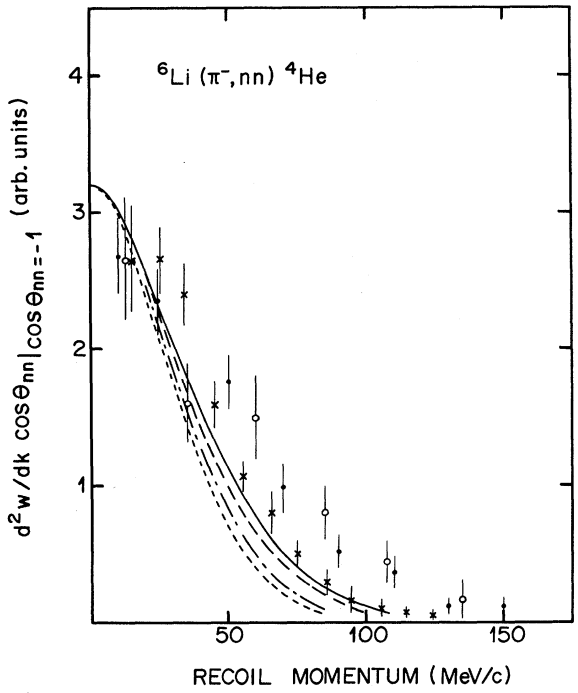

FIG. 14. The recoil momentum distribution of ^{4}He for the absorption of stopped negative pions by ^{6}Li. The dashed and solid curves are calculated with and without the cutoff approximation for the $2S$ state wave function by taking into account the contribution due to relative motion between two particles participated in the absorption. With the zero-range approximation for the absorption, these curves are reduced, respectively, to the dotted and dot-dashed ones. $R = 3.5$ fm is used. The experimental data ◆ are taken from Ref. 32 and those ϕ are from Ref. 33. The data obtained from the absorption of positive pions in flight (Ref. 3) are shown by $*$.

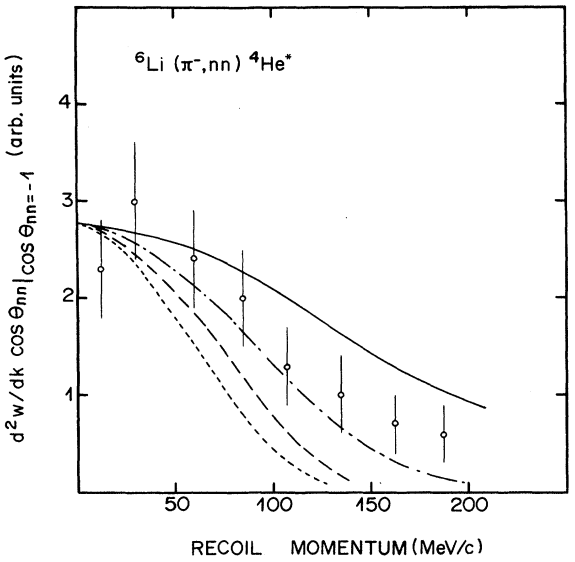

FIG. 15. The recoil momentum distribution of ^{4}He left in the positive parity states around 26 MeV excitation in the ^{6}Li$(\pi^-, 2n)^4$He* reaction. The dashed and solid curves are calculated, respectively, with and without the cutoff approximation for the 1S state wave function by including the contribution due to the relative motion between two particles participated in the absorption. With zero-range approximation, these curves are reduced, respectively, to the dotted and dot-dashed ones. $R=3.5$ fm is used. The data ϕ are taken from Ref. 33.

where E denotes the total energy of the particle corresponding to its suffix. Since the momentum conservation imposes

$$\vec{k}+\vec{K}=0\,, \tag{29}$$

$\vec{k}^2$ is complementary to $\vec{K}^2=\vec{k}^2$, where $\vec{K}$ is the recoil momentum of the residual nucleus.

Figures 14 and 15 show the momentum distributions for the recoil nucleus in its ground and highly excited states, respectively, compared with data.[32,33] The pion absorption by two particles in a deuteron cluster and in an α-particle cluster lead, respectively, to the residual nucleus left in these states. The results calculated by ignoring the contribution of the relative wave functions between the two particles differ appreciably from the results in which the relative wave functions are taken into account.

The width of the recoil momentum distribution calculated with Eq. (25) is broader than that with Eq. (27). The agreement between the calculated results and data in Fig. 14 is still not particularly satisfactory. However, it is worthwhile to note that the data are well reproduced with the use of the ϵ value for the three-body breakup of ^{6}Li into an α particle, a proton, and a neutron, instead of that for the two-body breakup into an α particle and a deuteron. This is shown in Fig. 16.

IV. DISCUSSION

A. Conventional cluster model wave function

The cluster model wave function is easily constructed in terms of harmonic oscillator functions. Only with these functions is the factorization of the c.m. and relative wave functions for clustering particles possible in analytic form.

For the d-α cluster model of ^{6}Li, the radial form of a 1D state wave function with an S state angular part

$$\phi(\vec{r})=Nr^2e^{-ar^2}Y_{00}(\hat{r}) \tag{30}$$

is often used by many authors[12,13] for describing the motion for the c.m. of one cluster with respect to that of the other. From the shell model point of view it is more reasonable, however, to use a 2S state wave function

$$\phi(\vec{r})=N(1-cr^2)e^{-ar^2}Y_{00}(\hat{r})\,, \tag{31}$$

which takes into account the requirement for a shell model node. After some straightforward calculations in Eq. (14), both functions (30) and (31) lead to antisymmetrized wave functions $\bar{\phi}(\vec{r})$ ex-

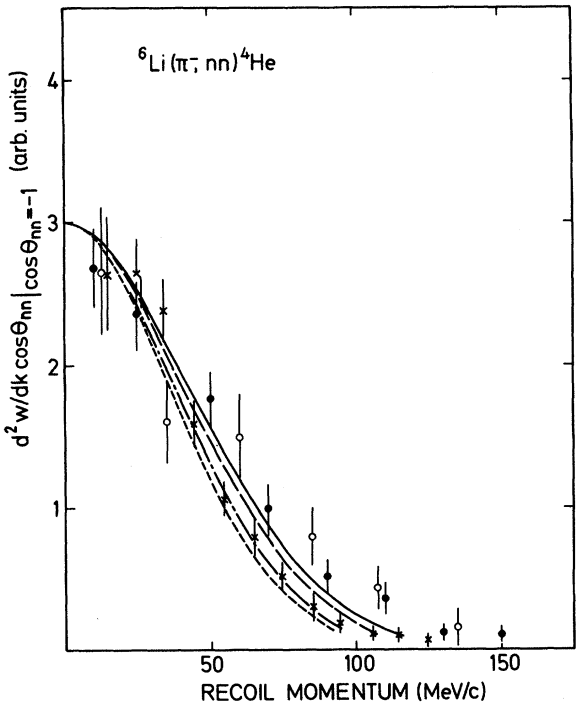

FIG. 16. The recoil momentum distribution of ^{4}He in the ^{6}Li$(\pi^-, nn)^4$He reaction. Except that the separation energy for the three-body break up of ^{6}Li is used, the curves correspond to those in Fig. 14.

pressible in terms of Gaussian functions. The wave functions $\tilde{\phi}(\vec{r})$ obtained from Eqs. (30) and (31) have an oscillatory structure in the interior region, although they are not identical. The function $\tilde{\phi}(\vec{r})$ derived with Eq. (31) seems to reproduce[14] the elastic and inelastic form factors obtained from electron scattering data better than that derived with Eq. (30).

The difference between the wave function given by Eq. (30) and $\tilde{\phi}(\vec{r})$ derived from it is large in the interior region. If one uses the nodeless wave function given by Eq. (30) without the antisymmetrization, the predicted cross section for the QFS is different from that calculated with the function $\tilde{\phi}(\vec{r})$. The diminution of the overlap integral due to the oscillatory structure of wave functions makes optical distortion effects for the incident and outgoing particles less important, compared with the case for the nodeless wave function. If the wave function given by Eq. (30) without the antisymmetrization is used to estimate the optical distortion effects, the effects are overestimated, compared with the case for the wave function given by Eq. (31). If the wave function given by Eq. (30) is used to see effects due to the antisymmetrization of particles in ^{6}Li, the effects become large, since $\tilde{\phi}(\vec{r})$ has a form of the $2S$ state function instead of the radial form of the $1D$ state function.

A similar situation exists for the t-α cluster model of ^{7}Li. The radial form of a $1F$ state wave function with a P state angular part

$$\phi(\vec{r}) = Nr^3 e^{-ar^2} Y_{1m}(\hat{r}) \tag{32}$$

is conventionally used for describing the motion of the c.m. of one cluster relative to that of the other. Instead, the use of a $2P$ state wave function

$$\phi(\vec{r}) = Nr(1 - cr^2) e^{-ar^2} Y_{1m}(\hat{r}) \tag{33}$$

is more justified, since this function satisfies the requirement for a shell model node. The antisymmetrized wave functions $\tilde{\phi}(\vec{r})$ obtained from Eqs. (32) and (33) have their oscillatory structure, although again they are not identical. The function given by Eq. (33) is similar to $\tilde{\phi}(\vec{r})$ derived with it. The function $\tilde{\phi}(\vec{r})$ derived with Eq. (32) differs completely from its original $\phi(\vec{r})$ in the interior region. If the wave function given by Eq. (32) is used to estimate the antisymmetrization effects of particles in ^{7}Li, they become large compared with the case of the wave function given by Eq. (33). The wave function given by Eq. (32) overestimates optical distortion effects for incident and outgoing particles, compared with the case for the wave function with a node given by Eq. (33).

The harmonic oscillator wave function has an inadequate tail, although the use of it is convenient. The function should be modified phenomenologically by matching it with a function having the correct asymptotic form. The contribution of the modified wave function to the overlap integral becomes relatively small for the inside of the matching radius, since its asymptotic part accounts for a large part of the cross section. This is especially the case for QFS with small separation energies.

The form factor for the elastic and inelastic scattering is the Fourier transform of the product of two bound state wave functions. This product falls off more rapidly with increasing radius and in addition does not give rise to such a cancellation as can occur in the overlap integral. Therefore, the asymptotic part of the wave function is less important for the form factor, compared with the overlap integral of QFS. This is the reason why the harmonic oscillator function can explain the elastic and inelastic form factors, inspite of its very poor asymptotic form which results in poor predictions for QFS data.

B. Momentum transfer dependence of x-y system

When the cross section $(d\sigma/d\Omega)_{x-y}$ depends strongly on the momentum transfer $\vec{\kappa} = \vec{\kappa}_i - \vec{\kappa}_f$, effects due to this variation of $(d\sigma/d\Omega)_{x-y}$ appear in the correlation cross section for the QFS. Here $\vec{\kappa}_i$ is the relative momentum between $\vec{k}_0$ and $-\vec{k}_B$ in the initial state, and $\vec{\kappa}_f$ is that between $\vec{k}_x$ and $\vec{k}_y$ in the final state. For the QFS kinematical conditions $\vec{\kappa}$ is close to $\vec{q}$. These effects are seen[34] in the correlation cross sections for the $(\alpha, 2\alpha)$ reaction since $(d\sigma/d\Omega)_{\alpha-\alpha}$ depends strongly on incident and transferred momenta.

For the QFS model, the dependence of the correlation cross section on $\vec{q}$ is assumed to be accounted for by the dependence of $(d\sigma/d\Omega)_{x-y}$ on $\vec{q}$. For the use of the wave function antisymmetrized with the method given by Eq. (14), the overlap between the internal wave functions of clustering particles $\phi_y(\vec{\rho}_y)$ and corresponding free particle $\psi_y(\vec{\rho}_y)$ has to be assumed to be constant and hence the correlation cross section divided by $K'(d\sigma/d\Omega)_{x-y}$ is a function of $\Delta\vec{k}$ only.

On the other hand, when the $A(x,xy)B$ reaction is considered from a microscopic point of view, the internal wave function $\phi_y(\vec{\rho}_y)$ gives the overlap which depends on the momentum transfer $\vec{q}$ as given by Eqs. (7) and (8). For the kinematical conditions that allow $\vec{q}$ to vary the correlation cross section is affected by the variation of the overlap. If the c.m. momentum distribution of clustering particles relative to the c.m. of the others in the nucleus is defined with the QFS cross section divided by $K'(d\sigma/d\Omega)_{x-y}$, the shape as well as the absolute value of such defined momentum

distribution vary with $\vec{q}$. This can be significant for the wave function $\phi_y(\vec{\rho}_y)$ which is very different from that for the corresponding free particle $\psi_y(\vec{\rho}_y)$.

However, the dependence of the correlation cross section on $\vec{q}$ can be minimized by choosing the kinematical conditions so as to fix $\vec{q}$. The shape of the correlation cross section becomes rather independent of $\vec{q}$ although its absolute value still depends on the $\vec{q}$ value chosen.

C. Final-state interaction effects

The relative energy between the particle y and residual nucleus B is rather low compared with those between x and y and between x and B, θ_x usually being chosen to be relatively small for the QFS kinematics. Thus the final-state interaction between y and B is expected to be important. However, if $\vec{q}$ is fixed by keeping the energy and scattering angle of x both constant, then the relative energy between y and B also remains constant. Hence, effects due to the final-state interaction hardly appear in the correlation cross section for QFS, as far as the relative energy does not exactly correspond to any resonance state between y and B. This is the case for the cross sections for the ^{6}Li$(p,pd)^4$He, ^{7}Li$(p,pt)^4$He, and ^{6}Li$(p,p^3$He$)^3$H reactions, shown in Figs. 1, 5 and 6, respectively. The relative energies of d-^{4}He, t-^{4}He, and ^{3}He-^{3}H systems are constant for the experimental conditions for these reactions at about 29, 16, and 13 MeV, respectively. If the relative energy coincides with a resonance state, the correlation cross section is affected by the angular dependence of the decaying mode for the resonant y-B system.

At low incident energies, of course, final-state interactions can have a very severe effect on the cross section.

When more than two α particles are produced in the reaction, attention should be paid to the strong interactions between α particles. The resonances act to modify the shape of the spectra and absolute values of the correlation cross section predicted with the simple spectator model. The cross section is enhanced in the kinematical region corresponding to the resonances, while the cross section for the QFS kinematic region is reduced. This is seen[34] in reactions such as ^{6}Li$(\alpha, \alpha d)^4$He, ^{9}Be$(\alpha, 2\alpha)^5$He, and ^{12}C$(\alpha, 2\alpha)^8$Be where the relative energy between α particles is allowed to vary in the chosen kinematical conditions.

D. Use of deuterons as projectiles

A priori the deuteron might be thought unsuitable as a projectile particle for QFS because of its weakly bound structure and easy dissociation. However, the experiment of Hagelberg, Haase, and Sakamoto[2] has shown that the correlation cross section for the ^{6}Li$(d, \alpha d)^2$H reaction is consistent with that for the ^{6}Li$(p,pd)^4$He reaction. The only difference comes from the kinematical factor and the cross section $(d\sigma/d\Omega)_{x-y}$. This shows that the overlap integral hardly depends on the kind of projectile because of the cancellation occurring in the interior region. The asymptotic part of $\phi(\vec{r})$ largely accounts for the correlation cross section for QFS in a reaction such as ^{6}Li$(d, \alpha d)^4$He. A particle, such as a deuteron, which easily looses its structure by nuclear interactions is very useful as a projectile for QFS, since the cutoff approximation is safely employed in the neglect of antisymmetrization effects of particles in the target nucleus.

E. "Clustering probability"

It might be concluded that the clustering structure is a surface phenomenon, on the basis of the apparent agreement between data and results calculated with the asymptotic function by introducing the cutoff approximation. However, before deriving such a conclusion attention should be paid to the fact that the overlap integral is diminished in the interior region, when the wave function has nodes. For analyzing data, some authors used a Hankel function which was normalized to be zero inside the cutoff radius by assuming that the clustering structure is a surface phenomenon. This is in all likelihood not true, as pointed out by Hagelberg *et al.*[2] The Hankel function with such a normalization predicted the shape of the spectra of the correlation cross sections which is very close to those calculated by taking account of the wave function for the interior region, because of the diminution of the overlap integral due to the oscillatory structure of the wave function in the region. However, it predicted too large cross sections.

The so-called clustering probability was found to vary over two orders of magnitude in early analyses of data for the breakup reaction of ^{6}Li into an α particle and a deuteron. These analyses, however, did not take into account the diminution of the overlap integral in the interior region nor the correct asymptotic form of the wave function.

The configuration of ^{3}He and t components in ^{6}Li is directly indicated[35,36] by reactions such as ^{3}H$(^3$He$, \gamma)^6$Li, ^{6}Li$(\gamma, ^3$He$)^3$H, ^{11}B$(^3$He$, ^6$Li$)^8$Be, and ^{7}Li$(^3$He$, \alpha)^6$Li. In contrast, the cross section for the ^{6}Li$(p,p^3$He$)^3$He is smaller than that for the ^{6}Li$(p,pd)^4$He reaction by a factor of 20 around $\Delta\vec{k}=0$ in QFS. This might have been surprising since the spectroscopic factor for the breakup into an α particle and a deuteron can be at most only $(\frac{a}{8})^2$ times[14,17] larger than that for the breakup into

a triton and a ^{3}He, as far as we believe in the shell model. This difference, however, is now simply explained[6] by reference to their greatly different ϵ values. The small cross section for the ^{6}Li-$(p,p^3\mathrm{He})^3$H reaction does not mean a small probability for the t-^{3}He configuration in ^{6}Li, but rather, mainly reflects the influence of a large ϵ value. It should be noted that the observed correlation cross sections for the ^{6}Li breakup reaction into a deuteron and an α particle can be well reproduced with the square well function of its normalization factor $c^2 = \theta_{d\alpha}{}^2 = 0.7$–$0.8$, although the most probable value of $\theta_{d\alpha}{}^2 = 1.07$ for harmonic oscillator cluster model wave functions is used in the present calculation. If $\theta_{d\alpha}{}^2 = 0.7$–$0.8$ is used, instead of 1.07, the ratio of $\theta_{t^3\mathrm{He}}{}^2 = 0.6$ to 0.7–0.8 is close to the value $(\frac{8}{9})^2$ obtained with the shell model.

F. Wave functions with many parameters

The use of more realistic functions such as a Woods-Saxon type may be suitable for calculating the cross sections. However, this is not essential for explaining the QFS data. The asymptotic behavior of the function dominates in the cross sections for QFS with small $\Delta\vec{k}$. The square well function gives the correct asymptotic form. Instead, the use of complicated wave functions with many parameters may easily cause the insight for the QFS process to be lost.

G. Large separation energies and large momentum transfers

The contribution to the overlap integral from the interior region increases for the reaction involving a large ϵ value. The optical distortions for the incident and outgoing particles can attenuate the overlap integral. However, this attenuation is unimportant because of the diminution of the overlap integral due to the oscillatory structure of the wave function.

When the wave function has no node, attention should be paid to the attenuation of the overlap integral due to the optical distortions. The diminution of the overlap integral for the interior region does not occur. It would be interesting the measure cross sections for reactions involving large ϵ values and residual nucleus left in highly excited states to study the attentuation of the overlap integral.

Information about the wave function in the interior region may be obtained from the study of cross sections involving large $\Delta\vec{k}$, but these have generally not yet been measured with high precision. However, the spectrator model is suspected not to be valid for describing phenomena involving large $\Delta\vec{k}$.

H. Recoil momentum distribution by pion absorption

The recoil momentum distribution of B in the $A(x,xy)B$ reaction is dominated by the c.m. wave function of clustering particles y. The relative wave functions in the particle y have little effect on the shape of the spectra for the correlation cross section, although they can participate weakly in fixing the absolute values of the cross sections. In contrast, the c.m. as well as relative wave functions of the particles participating in the pion absorption take part in determining the shape of the recoil momentum distribution. The width of the recoil momentum distribution for the latter is, in general, broader than that for the former. Together with the c.m. wave function of clustering particles reproducing the QFS data, information on the relative wave functions of the clustering particles can be extracted from the recoil momentum distribution resulting from the pion absorption.

V. CONCLUSIONS

The cross section for the QFS on clustering particles y in the $A(x,xy)B$ reaction is explained in terms of the separation energy ϵ of the particles y from the nucleus. The ϵ value indicates the ease of removal of the particles from the nucleus, a small value ϵ leading to a large cross section.

The wave function for the c.m. of the particles y relative to that of remaining particles has generally high principal quantum numbers when the residual nucleus is left in its ground and lower excited states. The wave function with its high principal quantum number has an oscillatory structure. The overlap integral is canceled in the interior region. The asymptotic part of the wave function with a small ϵ value accounts for the spectrum of the correlation cross section in its shape and even in its absolute value. However, even if the cross section is mostly due to the asymptotic part of the wave function, this does not mean that the wave function is null in the interior region.

The oscillatory structure of the wave function cancels the overlap integral for the interior region and makes effects due to the nuclear absorptions for the incident and outgoing particles less important compared with the case for the nodeless wave function. Hence, the cross sections divided by the kinematical factor and x-y scattering cross section $(d\sigma/d\Omega)_{x-y}$ hardly depend on the kind of projectile particle, if its energy is high enough, and when the kinematical conditions are chosen so that final-state interactions do not strongly appear.

The overlap integral calculated with a wave function having the correct asymptotic form has little ambiguity when cancellation occurs in interior region. If this is the case, it can hardly be expected that information about the wave function can be extracted from data for the QFS where Eq. (9) is valid, besides information already contained in the separation energies. However, the spectroscopic factor for particles in the nucleus, that is, the square of the fractional parentage coefficient multiplied by the overlap between the internal wave functions of clustering and free particles, can be extracted within a narrow margin by comparison of the observed cross section and the value predicted with the wave function having the correct asymptotic form. This is especially useful for the case of a zero-angular momentum state for the c.m. motion of the clustering particles, since the cross section measured only at zero momentum transfer $\Delta\vec{k}=0$ is sufficient to extract the factor.

The authors wish to express their gratitude to Dr. E. L. Haase and Dr. C. W. Lewis for their interest in the present work as well as for many valuable discussions. They also wish to record their appreciation of the support of Professor A. Citron. One of us (Y.S.) is greatly indebted to Professor E. Schopper for his kind hospitality extended to him.

---

*Research supported in part by the Alexander von Humboldt-Stiftung.

†Visitor at Nuclear Physics Division, CERN, Geneva.

[1]P. Cüer, Phys. Rev. 80, 906 (1950); P. Cüer and A. Samman, J. Phys. (Paris) 19, 15 (1958).

[2]R. Hagelberg, E. L. Haase, and Y. Sakamoto, Nucl. Phys. A207, 366 (1973).

[3]K. Baehr, T. Becker, O. M. Bilaniuk, and R. Jahr, Phys. Rev. 178, 1706 (1969).

[4]J. Favier, T. Bressani, G. Charpack, L. Massonet, W. E. Meyerhof, and C. Zupancic, Nucl. Phys. A169, 540 (1971).

[5]A. K. Jain, N. Sarma, and B. Banerjee, Nucl. Phys. A142, 330 (1970).

[6]Y. Sakamoto, P. Cüer, and F. Takéutchi, Phys. Rev. C 9, 2440 (1974).

[7]Y. Sakamoto and T. Sasakawa, Prog. Theort. Phys. 21, 879 (1959).

[8]Y. Sakamoto, Nuovo Cimento 28, 207 (1963); Phys. Rev. 134, B1211 (1964).

[9]D. F. Jackson, Rev. Mod. Phys. 37, 393 (1965).

[10]It should be noted that, even if $\vec{q}$ is kept to be constant, the ratio is in general not unity and it takes part in determining the absolute values of cross sections calculated. This is due to the fact that the internal wave functions of clustering particles differ from those of corresponding free particles.

[11]D. F. Jackson, in *Advances in Nuclear Physics*, edited by M. Baranger and E. Vogt (Plenum, New York, 1971), Vol. 4.

[12]Y. C. Tang, K. Wildermuth, and L. D. Pearlstein, Phys. Rev. 123, 548 (1961).

[13]K. Wildermuth and W. McClare, *Springer Tracts in Modern Physics* (Springer, New York, 1966), Vol. 41.

[14]Yu. A. Kudeyarov, E. V. Kurdyumov, V. G. Neudatchin, and Yu. F. Smirnov, Nucl. Phys. A163, 316 (1971).

[15]A. Johansson and Y. Sakamoto, Nucl. Phys. 42, 625 (1963); G. Jacob and T. Berggren, *ibid.* 47, 481 (1963).

[16]For example, A. N. Boyarkina, Izv. Akad. Nauk. SSSR, Ser. Fiz. 28, 337 (1964); I. Rotter, Fortschritte Phys. 16, 195 (1968); S. Cohen and D. Kurath, Nucl. Phys. A141, 143 (1970).

[17]P. Kramer and M. Moshinsky, in *Group Theory and Its Applications*, edited by F. Loebl (Academic, New York, 1968).

[18]Y. Nishida, Nucl. Phys. 82, 385 (1966).

[19]K. Kuroda, A. Michalowicz, and M. Poulet, Nucl. Phys. 88, 33 (1966); O. Chamberlain and M. O. Stern, Phys. Rev. 94, 666 (1954); H. Langevin-Joliot, P. Narboni, J. P. Didelez, G. Duhamel, L. Marcus, and M. Roy-Stephan, Nucl. Phys. A158, 309 (1970); A. M. Carmack, J. N. Palmieri, N. F. Ramsey and R. Wilson, Phys. Rev. 115, 599 (1959).

[20]D. Bachelier, thèse d'Etat, Faculté des Sciences, Orsay, 1971 (unpublished).

[21]C. Ruhla, M. Riou, M. Gusakow, J. C. Jacmart, M. Liu, and L. Valentin, Phys. Lett. 6, 282 (1963).

[22]I. A. Mackenzie, S. K. Mark, and T. Y. Li, Nucl. Phys. A178, 225 (1971).

[23]D. Bachelier, M. Bernas, C. Détraz, P. Radvanyi, and M. Roy, Phys. Lett. 26B, 283 (1968).

[24]J. F. Jackson and L. R. B. Elton, Proc. Phys. Soc. 85, 659 (1965).

[25]V. V. Balashov and V. I. Mazkov, Nucl. Phys. A163, 465 (1971).

[26]S. C. Wright, Phys. Rev. 99, 996 (1955).

[27]L. Valentin, Nucl. Phys. 62, 81 (1965).

[28]R. M. Hutcheon, O. Sundberg, and G. Tibell, Nucl. Phys. A154, 261 (1970).

[29]D. Bachelier, M. Bernas, O. M. Bilaniuk, J. L. Boyard, J. C. Jourdain, and P. Radvanyi, Phys. Rev. C 7, 165 (1973).

[30]Y. Sakamoto, Nucl. Phys. 87, 414 (1966); Nuovo Cimento 37, 774 (1965).

[31]L. R. B. Elton, *Nuclear Sizes* (Oxford U. P., London, 1961).

[32]H. Davies, H. Muirhead, and J. N. Woulds, Nucl. Phys. 78, 663 (1966).

[33]F. Calligaris, C. Cernigoi, L. Gabrielli, and F. Pellegrini, Nucl. Phys. A126, 209 (1969); J. W. Watson, H. G. Pugh, P. G. Roos, D. A. Goldberg, R. A. J. Riddle, and D. I. Bonbright, *ibid.* A172, 513 (1973).

[34]J. R. Pizzi, M. Gaillard, P. Gaillard, A. Guichard, M. Gusakow, R. Reboulet, and C. Ruhla, Nucl. Phys. A136, 496 (1969); E. Velten, Doktorarbeit, Fakultät für Physik, Universität Karlsruhe, 1969 (unpublished);

Kernforschungszentrum, Karlsruhe, External Report No. 3/69/24, 1970 (unpublished).
[35]A. M. Young, S. L. Blatt, and R. G. Seyler, Phys. Rev. Lett. 25, 1764 (1970).
[36]M. F. Werby, M. B. Greenfield, K. W. Kemper, D. L. McShan, and S. Edwards, Phys. Rev. C 8, 106 (1973).